

# Malaria temporal dynamic clustering for surveillance and intervention planning

Eva Legendre<sup>1</sup>, Laurent Lehot<sup>1</sup>, Sokhna Dieng<sup>1</sup>, Stanislas Rebaudet<sup>1,2</sup>, Aung Myint Thu<sup>3</sup>, Jade D Rae<sup>3,4,5</sup>, Gilles Delmas<sup>3,5</sup>, Florian Girond<sup>6,7</sup>, Vincent Herbreteau<sup>6</sup>, François Nosten<sup>3,5</sup>, Jordi Landier<sup>1,3</sup> \*, Jean Gaudart<sup>1,8</sup> \*.

1. Aix Marseille Univ, IRD, INSERM, SESSTIM, Aix Marseille Institute of Public Health, ISSPAM, Marseille, France
2. Hôpital Européen Marseille, Marseille, France
3. Shoklo Malaria Research Unit, Mahidol Oxford Tropical Medicine Research Unit, Mae Sot, Thailand
4. Mahidol-Oxford Tropical Medicine Research Unit, Faculty of Tropical Medicine, Mahidol University, Bangkok, Thailand
5. Centre for Tropical Medicine and Global Health, Nuffield Department of Medicine Research building, University of Oxford Old Road campus, Oxford, UK
6. Institut de Recherche pour le Développement, UMR 228 Espace-Dev (IRD, UA, UG, UM, UR), Phnom Penh, Cambodia.
7. Institut Pasteur du Cambodge, Phnom Penh, Cambodia.
8. La Timone Hospital, BioSTIC, Biostatistics and ICT, Marseille France

\*, authors contributed equally to the article

Corresponding author: Eva Legendre; [eva.legendre@univ-amu.fr](mailto:eva.legendre@univ-amu.fr); +33 (0)6 89 63 12 32 ;  
27 boulevard Jean Moulin, 13005 Marseille, France

## Abstract

**Background.** Targeting interventions where most needed and effective is crucial for public health. Malaria control and elimination strategies increasingly rely on stratification to guide surveillance, to allocate vector control campaigns, and to prioritize access to community-based early diagnosis and treatment (EDT). We developed an original approach of dynamic clustering to improve local discrimination between heterogeneous malaria transmission settings.

**Methods.** We analysed weekly malaria incidence records obtained from community-based EDT (malaria posts) in Karen/Kayin state, Myanmar. We smoothed longitudinal incidence series over multiple seasons using functional transformation. We regrouped village incidence series into clusters using a dynamic time warping clustering and compared them to the standard, 5-category annual incidence standard stratification.

**Results.** We included 1,115 villages from 2016 to 2020. We identified eleven *P. falciparum* and *P. vivax* incidence clusters which differed by amplitude, trends and seasonality. Specifically the 124 villages classified as “high transmission area” in the standard *P. falciparum* stratification belonged to the 11 distinct groups when accounting to inter-annual trends and intra-annual variations. Likewise for *P. vivax*, 399 “high transmission” villages actually corresponded to the 11 distinct dynamics.

**Conclusion.** Our temporal dynamic clustering methodology is easy to implement and extracts more information than standard malaria stratification. Our method exploits longitudinal surveillance data to distinguish local dynamics, such as increasing inter-annual trends or seasonal differences, providing key information for decision-making. It is relevant to malaria strategies in other settings and to other diseases, especially when many countries deploy health information systems and collect increasing amounts of health outcome data.

**Funding.** The Bill & Melinda Gates Foundation, The Global Fund against AIDS, Tuberculosis and Malaria (the Regional Artemisinin Initiative) and the Wellcome Trust funded the METF program.

NOTE: This preprint reports new research that has not been certified by peer review and should not be used to guide clinical practice.

## 51 Key words

52 Seasonal malaria; temporal dynamics; clustering

53

54

## 55 Introduction

56 During malaria control or pre-elimination phases, the World Health Organization (WHO)  
57 recommends countries to rely on a stratification process in order to allocate resources and  
58 interventions. Stratification aims to produce discrete maps differentiating areas based on transmission  
59 intensity and receptivity.<sup>1</sup> Transmission intensity can be measured directly by entomological  
60 parameters (entomological inoculation rate) but require extensive efforts and significant resources.<sup>2,3</sup>  
61 In practice, clinical malaria incidence over one year, also called “annual parasite incidence” (API) is  
62 often used as a proxy of transmission. Receptivity is a complex concept without a straightforward  
63 quantitative measurement.<sup>3</sup> In the context of prevention of reintroduction, it mainly refers to the ability  
64 of an ecosystem to enable malaria transmission even if it is not ongoing: presence of competent  
65 vectors, suitable climate and susceptible population.<sup>1</sup> Vectorial capacity can provide important insights  
66 on receptivity, but due to lack of large scale entomological information, receptivity is often  
67 approximated using environmental (meteorological/landscape) data.<sup>1,3</sup> Depending on data availability,  
68 stratification can be performed from broad (region, district) to fine (village, health area) geographical  
69 scales to fit operational needs.

70 In the Greater Mekong Subregion (GMS), malaria persists in some high transmission foci where  
71 *Plasmodium falciparum* and *P. vivax* are responsible of most morbidity and mortality.<sup>4</sup> *P. falciparum*  
72 elimination in this area has been prioritized in response to the emergence of artemisinin resistance.<sup>4-  
73 6</sup>

74 Myanmar remains the country with the highest malaria burden in the GMS, especially in mountainous  
75 borderlands. In accordance with WHO technical guidelines, Myanmar planned its 2016–2030 elimination  
76 strategy relying on API to stratify its regions and townships for operational planning.<sup>7</sup> Townships are  
77 not the finest administrative division in Myanmar; it is subdivided in village tracts and villages. This  
78 stratification method is easily implemented based on routine data collections but the stratification may  
79 not be sufficient to adapt and optimize surveillance and intervention. When malaria control progresses,  
80 malaria transmission becomes increasingly heterogeneous and unstable, for example due to local  
81 differences in the environment sustaining transmission or in the impact of interventions. The complex  
82 settings of malaria elimination also imply sporadic epidemics, more unexpected temporal dynamics  
83 not addressed with classical approaches, and need to assess the whole time series evolution. To  
84 consider this variability, it is necessary to develop tools that describe more accurately malaria  
85 dynamics over several years.

86 According to WHO and Myanmar NMCP report in 2015, stratification at township level identifies Karen  
87 state mostly as a moderate transmission area with high risk in the northern township.<sup>8</sup> This state,  
88 located at the Myanmar–Thailand border, is a typical GMS elimination setting combining low incidence  
89 areas with persisting high transmission hotspots. In this state, the Malaria Elimination Task Force  
90 (METF) was launched in 2014. The program offered early diagnostic and treatment in over 1200 malaria  
91 posts (MPs) in four townships and targeted mass drug administration (MDA) in selected high  
92 prevalence village.<sup>9,10</sup> It offered the opportunity to describe malaria heterogeneity at a finest  
93 geographical scale operationally relevant – the village.

94 This study proposed a method which allow stratification in settings where multiple, different malaria  
95 seasonality coexists, and where epidemiology and dynamics can change due to interventions or  
96 environmental drivers. We compared two malaria incidence stratifications (routine standard versus  
97 temporal dynamic clustering method) to discriminate malaria transmission settings at village scale.  
98 The temporal dynamic clustering method aimed to identify hotspots of transmission and temporal  
99 dynamics heterogeneities at village scale over several years and for each malaria species. It will help  
100 to further understand malaria epidemiology in the Karen state and optimize surveillance and  
101 interventions beyond conventional API-based stratification. This required to analyse hundreds of  
102 heterogeneous time series simultaneously without statistical assumptions. We propose a temporal  
103 dynamic clustering methodology to overcome this methodological hurdle.

104  
105

## 106 Method

### 107 *Study design and setting*

108 In this study, we analysed longitudinal records of *P. falciparum* and *P. vivax* malaria cases by malaria  
109 post (MP) of the Malaria Elimination Task Force (METF), between 2016 and 2020 in the Karen state of  
110 Myanmar along the Thailand border. 95% of villages identified in the target region hosted a malaria  
111 post, the vast majority opening between May 2014 and August 2016 (n=1057, 95%).<sup>11</sup> MP systematically  
112 tested fever cases using a *P. falciparum*-*P. vivax* rapid diagnostic test (RDT) and sent weekly reports  
113 specifying the number of *P. falciparum* and *P. vivax* cases diagnosed.<sup>9</sup> At the time of the analysis,  
114 malaria records were available until March 2020.

115

### 116 *Data of malaria incidence rate*

117 For each village, we estimated *P. falciparum* and *P. vivax* observed incidence as the weekly or annual  
118 case count recorded by MPs divided by the village population during study period. The population was  
119 estimated using the number of households in the village and an average of 5 members per household  
120 according to Myanmar census data.<sup>12</sup>

121

### 122 *Malaria stratification on annual parasite incidence (API) in 2019*

123 For each village, API was calculated as the sum of malaria cases in a year divided by the number of  
124 people at risk in a year and reported as cases per 1000 person.year at risk. Following WHO GMS  
125 guidelines, Myanmar national plan for malaria elimination distinguished 5 strata based on API (*P.*  
126 *falciparum* and *P. vivax* cases combined) in 2019: transmission free area (API=0 /1000 individuals under  
127 surveillance for more than 3 years), potential transmission area (API=0), low transmission area (API<1),  
128 moderate transmission area (API between 1-5) and high transmission area (API>5).<sup>7,13</sup>

129

### 130 *Statistical analysis: the temporal dynamic clustering*

131 In the region, malaria is seasonal with patterns which could vary between areas and time. The objective  
132 of the temporal dynamic clustering method is to group malaria dynamics with similar seasonality,  
133 amplitude, shape, and by associating malaria outbreaks occurring in the same season. The method  
134 includes 3 successive steps: 1/ functional transformation to smooth time series; 2/ dynamic time

135 warping (DTW) metric calculation on functional data; 3/ partitioning around medoid (PAM) clustering  
136 on DTW matrix (Sup. Fig. 1).

137 The development of the temporal dynamic clustering responded to 3 challenges. First, the clustering  
138 method needed to consider not only amplitude but also malaria seasonality (i.e. intra-annual  
139 variability), curve shape, and allowing time lags to associate outbreaks occurring with few weeks of  
140 interval during the same season. Based on our previous comparison of metrics in the context of  
141 malaria, DTW metric was the most appropriate.<sup>14</sup> Second, DTW algorithm performance is sensitive to  
142 sharp irregularities.<sup>15</sup> Malaria time series at village scale were sharp and noisy, and required  
143 smoothing. In this complex elimination setting, environmental changes (meteorological, landscape,  
144 etc.), socio-political events or METF interventions occurrence induced differential dynamic variations  
145 and invalidated the stationarity assumption. It prevented the use of classical time series methods (e.g.  
146 ARIMA). Functional data transformation allowed to remove sharp irregularities, with smoothing  
147 parameters identical and optimized to the entire set of time series, and without stationarity  
148 assumptions.

149 Analyses were conducted using R 4.0 (R Development Core Team, R Foundation for Statistical  
150 Computing, Vienna, Austria) and {fda}, {TScust} and {dtw} packages. An R script is available in  
151 supplementary material to facilitate the implementation of the clustering method (Sup. Met. 1).

152

#### 153 Preliminary settings: village and time frame selection

154 We grouped cases and population denominators from MPs located less than 500m away from each  
155 other in “villages” - the statistical unit of this study.

156 Simultaneous functional transformation required time series with identical length. Because of MP  
157 were set up gradually, we selected a common study period based on calendar dates. We chose the  
158 period to include a maximal number of villages having at least one malaria case and to yield the period  
159 with the longest possible duration.

160 We excluded villages with more than two missing successive weekly report (>1% missing data) from  
161 the analysis. For villages with less than two consecutive weeks missing, we imputed missing weekly  
162 reports by the average of the number of cases from the following and the previous weeks. Missing  
163 reports were due to omission, phone network problem, problem of access, loss of the report, etc. We  
164 excluded villages without population denominator (missing household count) from the analysis.

165

#### 166 1/ Smoothing malaria time series using functional data transformation

167 Incidence time series were sharp, noisy, and sometimes seasonal. We used functional data to smooth  
168 simultaneously all the time series. For each time series, we estimated a function from its observed  
169 values. Every  $y$  time series of  $i$  weeks was transformed by a smooth function  $x(t)$ , which was a linear  
170 combination of elementary function, i.e. cubic B-splines, and an error term (Equation 1, 2). Cubic B-  
171 splines functions were grouped in a function basis  $\phi_k(t)$  containing  $k$  functions. As recommended, the  
172 number of functions  $k$  was equal to the number of weeks included in the study period.<sup>16</sup> Coefficients  $c$   
173 were estimated by minimizing the penalized (PEN) sum of squared errors (SSE) (Equation 3). The  
174 penalty was on the roughness of the function  $x(t)$  (i.e. measures the curvature of the curve). The  
175 smoothing parameter  $\lambda$ , indicating the emphasis of the penalization, was optimized by minimizing the  
176 sum of the GCV criterion of all  $v$  villages using a set of values of  $\log(\lambda)$  ranging from 0 to 10 with a step  
177 of 0.25 (Equation 4).<sup>16</sup>

178 Equation 1.  $y_i = x(t_i) + \varepsilon_i$

179 Equation 2.  $x(t_i) = \sum_{k=1}^k c_k \phi_k(t_i)$

180 Equation 3. 
$$F(c) = \underbrace{\sum_{i=1}^n [y_i - x(t_i)]^2}_{\text{SSE}} + \underbrace{\lambda \int (x''(t))^2 dt}_{\text{PEN}}$$

181  
182  
183 Equation 4.  $\lambda_{\text{optimal}} = \arg \min (\sum_{v=1}^V \text{GCV}_v)$ , with  $\text{GCV}(\lambda) = \left(\frac{n}{n-\text{df}(\lambda)}\right) \left(\frac{\text{SSE}}{n-\text{df}(\lambda)}\right)$

184 A square root transformation was applied before functional transformation to the incidence rate time  
185 series because of large-scale amplitude to the incidence rates.<sup>14</sup>

186  
187 2/ Distance between functional time series using the DTW metric

188 The dynamic time warping metric is a flexible metric, which distinguished two time series according  
189 to their amplitude and phases by considering time lags. The algorithm calculated distance between  
190 two villages after compressing or stretching functional time series locally to make them as similar as  
191 possible. This metric can be parametrized to specify the time-window of the stretch. We chose a three  
192 months window to associate malaria outbreaks belonging to the same transmission season (cold or  
193 rainy season).<sup>17,18</sup>

194  
195 3/ PAM clustering on DTW matrix

196 We applied partitioning around medoid (PAM) clustering to the distance matrix calculated with the DTW  
197 metric. PAM algorithm is similar to the k-means algorithm, except that the centre of each class, called  
198 “medoid”, corresponds to an observed time series and it is compatible with the DTW metric (i.e. a non-  
199 Euclidian distance).<sup>19-21</sup> We named each cluster based on visual assessment of its distinctive  
200 characteristics.

201 Minimization of the intra-class inertia average (I) and parsimony principle determined the optimal  
202 number of clusters G. The conditional intra-class inertia (CI) was estimated for each G cluster by the  
203 average of the DTW distance between the n villages (v) included in the cluster and its medoids (M)  
204 (Equation 5).

205  
206 Equation 5.  $I = \frac{\sum_{g=1}^G \text{CI}_g}{G}$  with  $\text{CI}_g = \frac{\sum_{l=1}^{n_g} d^2(v_l, M_g)}{n_g}$

207  
208 *Sensitivity analysis*

209 Simple approaches to improve API stratification were (i) to divide the "high transmission area"  
210 category (>5 cases/1000py) in sub-categories and (ii) to consider stratification results over several  
211 years. We compared our temporal dynamic clustering with a third stratification from 2016 to 2019 based  
212 on API stratification but subdividing the high transmission area category according to incidence  
213 quartiles.

214  
215

216 **Results**

217 *API stratification for Myanmar in 2019*

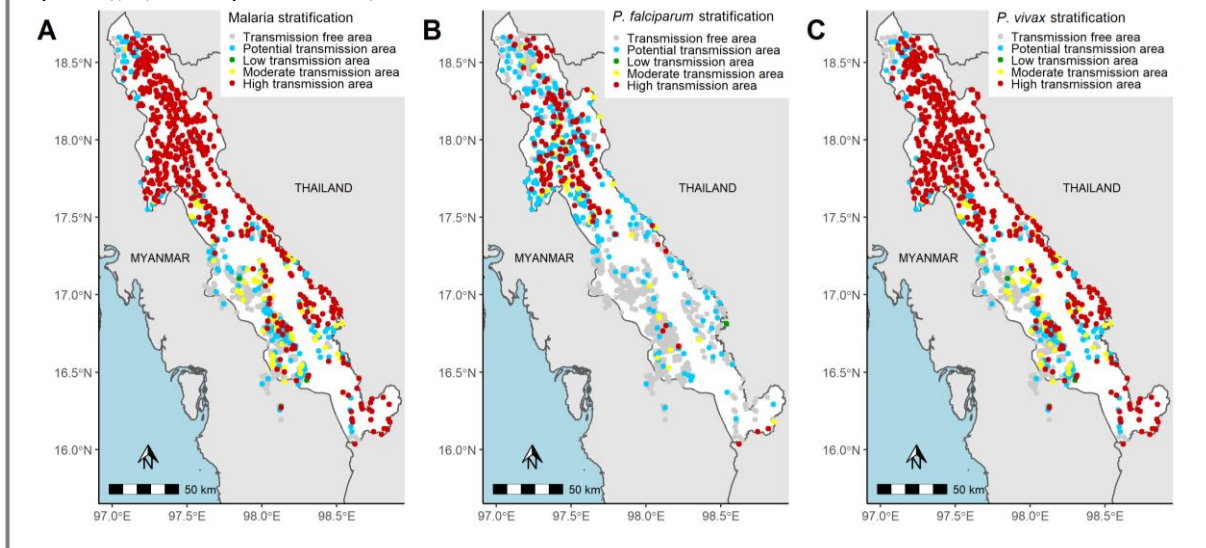
218 Since 2014, 1,205 MPs were set up by the METF program and were grouped in 1,115 villages spreading  
219 over 4 townships. In 2019, 1,032 villages had active MP reporting. The median population in the villages  
220 was 200 and the IQR was 115-360. For the Northern township where most malaria cases occurred, the  
221 median village population was 142 (IQR=95-215).

222  
223  
224  
225  
226  
227  
228  
229  
230  
231  
232  
233  
234  
235  
236  
237  
238  
239  
240  
241  
242  
243  
244  
245  
246  
247  
248  
249  
250  
251  
252  
253  
254  
255  
256  
257  
258  
259  
260  
261  
262  
263  
264  
265  
266  
267  
268  
269  
270  
271  
272  
273

Table 1. Annual parasite incidence (API, equivalent to annual malaria cases incidence /1000 individuals under surveillance) stratification in 2019 at village level. N(%).

	Malaria (both species)	<i>P. falciparum</i>	<i>P. vivax</i>
Transmission free area (API=0 for more than 3 years)	298 (28.9)	586 (57.1)	324 (31.4)
Potential transmission area (API=0)	167 (16.2)	250 (24.4)	154 (14.9)
Low transmission area (API<1)	3 (0.3)	1 (0.1)	3 (0.3)
Moderate transmission area (API=1-5)	65 (6.3)	40 (3.9)	64 (6.2)
High transmission area (API>5)	499 (48.4)	149 (14.5)	487 (47.2)

Figure 1. Map of API stratification on annual parasite incidence in 2019 at village level for A) malaria (both species), B) *P. falciparum* and C) *P. vivax*.



According to API stratification on both malaria species in 2019, 48.4% (n=499) of the villages corresponded to a high transmission area and 28.9% (n=298) to a transmission-free area. Taking into account only *P. falciparum* cases, the proportion of villages in a transmission-free area increased to 57.1%, twice more than in the overall malaria stratification. On the contrary, the proportion of villages in a high transmission area were divided by more than 3 to reach 14.5%. Considering *P. vivax* only, proportions were similar to the overall malaria stratification. This implied that malaria stratification is driven by *P. vivax* cases, which represented 91.9% of the total malaria burden (Tab. 1 & Fig. 1).

## Temporal dynamic clustering

### Village and study period selection

Seven villages without population denominator were excluded. The period from March 2016 to February 2020 maximized the number of villages included and the time series duration, with 676 villages followed over 206 weeks. Fourteen villages with >2 successive missing reports were excluded. Missing reports occurred rarely over time and villages (118 missing of 136,372 reports expected, i.e. 0.086%). The analysis included 662 villages (Sup. Fig. 2). Of 662 villages, 16.2% (n=107) belonged to the malaria transmission free stratum, 16.3% (n=108) belonged to the potential transmission stratum, 0.1% (n=1) to low, 5.9% (n=39) to moderate and 61.5% (n=407) to high transmission area strata.

274 *P. falciparum* clustering

275 The 662 *P. falciparum* incidence rate time series were simultaneously transformed into functional data  
276 ( $k=206$ ,  $\lambda=100$ ,  $GCV=196$ ). The temporal dynamic clustering identified 11 clusters (intra-class inertia=104)  
277 (Sup. Fig. 3).

278 Most villages (81%,  $n=539$ ) belong to the “very low” cluster, with a near zero *P. falciparum* incidence  
279 between 2016 and 2020. The “low” cluster regrouped 46 (7%) villages with sporadic cases and a low  
280 incidence rate. Two clusters exhibited an incidence peak during the rainy season in 2017 (0.8%,  $n=5$ ) or  
281 2018 (2%,  $n=13$ ). 40 villages exhibited a single incidence peak during the cold season and were grouped  
282 in three clusters according to the year: 2016 (2.7%,  $n=18$ ), 2017 (2.6%,  $n=17$ ) or 2018 (0.8%,  $n=5$ ). One  
283 cluster including 10 villages (1.5%) presented a decreasing trend with peaks in both cold and rainy  
284 seasons. Two clusters regrouped villages with a high incidence rate until September 2018 ( $n=5$  or 0.8%  
285 and  $n=3$  or 0.5%). The 11<sup>th</sup> cluster corresponded to a single village (Fig. 2).

286 When compared to API stratification, *P. falciparum* dynamic clustering distinguished villages according  
287 to both their current and previous incidence. Within the potential transmission stratum, the clustering  
288 distinguished villages with a consistently low incidence ( $n=22$ ) from villages where incidence recently  
289 dropped after persisting at high levels (hotspot,  $n=2$ ). Likewise, it identified 4 patterns in the high  
290 transmission stratum: 54 villages with a past incidence near zero, 36 villages with a past single  
291 outbreak, 6 villages with a decreasing tendency and 6 hotspots (Tab. 2).

292

293 *P. vivax* clustering

294 The 662 *P. vivax* incidence rate series were simultaneously transformed into functional data ( $k=206$ ,  
295  $\lambda=562$ ,  $GCV=487.5$ ). The temporal dynamic clustering identified 11 clusters ( $I=227$ ) (Sup. Fig. 3).

296 A majority of villages (69%,  $n=457$ ) belonged to the “very low” incidence cluster across the study period.  
297 Two clusters presented a low incidence rate. One presented sporadic cases across years ( $n=69$ , 10%),  
298 whereas the other displayed an increasing trend ( $n=45$ , 7%). Two clusters exhibited a marked  
299 seasonality in the rainy season and were distinguished by their trend: one decreased over time ( $n=13$ ,  
300 2%), whereas the other increased ( $n=23$ , 3.5%). A cold-season cluster was also identified ( $n=31$ , 5%),  
301 with its highest incidence during the 2017-18 cold season. Another cluster showed a low incidence until  
302 the end of 2017 and a rapid increase to a higher incidence rate after ( $n=14$ , 2%). One cluster identified  
303 villages with persistent cases ( $n=7$ , 1%). Finally, three clusters isolated individual villages (Fig. 3).

304 When compared to Myanmar API stratification, *P. vivax* dynamic clustering identified 10 different  
305 patterns within the high transmission stratum according to past incidence amplitude, tendency, and  
306 seasonality. Conversely, the “very low” cluster included the other 4 strata. (Tab. 3)

307

308 Geographical distribution of *P. falciparum* and *P. vivax* clusters

309 All but one villages which did not belong to the “very low” cluster of *P. falciparum* incidence were  
310 grouped in the Northern part of the Karen state with one specific group at the extreme north (in yellow)  
311 corresponding to an outbreak in cold season 2018-19 (Fig. 4A). *P. falciparum* hotspots villages (in  
312 orange and pink) were concentrated in another specific area.

313 Concerning *P. vivax*, villages which did not belong to the “very low” cluster of incidence were also  
314 grouped in the Northern part and along the Thailand-Myanmar border (Fig. 4B). Villages with a *P. vivax*  
315 increasing or persistent tendency (in pink, yellow, orange and red) were mostly localized in the  
316 Northeast part with a core composed of villages with a brutal incidence increasing in 2018 (in orange)  
317 or with persisting high incidence (in red). Another substantial aggregation of villages is present in the  
318 Southeast region with one *P. vivax* annual peak only in rainy season and with a decreasing tendency  
319 (in turquoise). Temporal dynamic clustering thus led to relevant spatial distribution of clusters.

320  
321  
322  
323  
324  
325  
326  
327  
328  
329  
330  
331  
332  
333  
334  
335  
336  
337  
338  
339  
340  
341  
342  
343  
344  
345  
346  
347  
348  
349  
350  
351  
352  
353  
354  
355  
356  
357  
358  
359  
360  
361  
362  
363  
364  
365

Figure 2. *P. falciparum* clustering. Temporal dynamic clustering identified eleven clusters. Black line corresponds to the central village (medoid) of each cluster. Coloured lines represent functional incidence rate of all villages included in the cluster across study period. When clusters contained only one village, only the medoid (black line) is presented corresponding to the time series of the village.

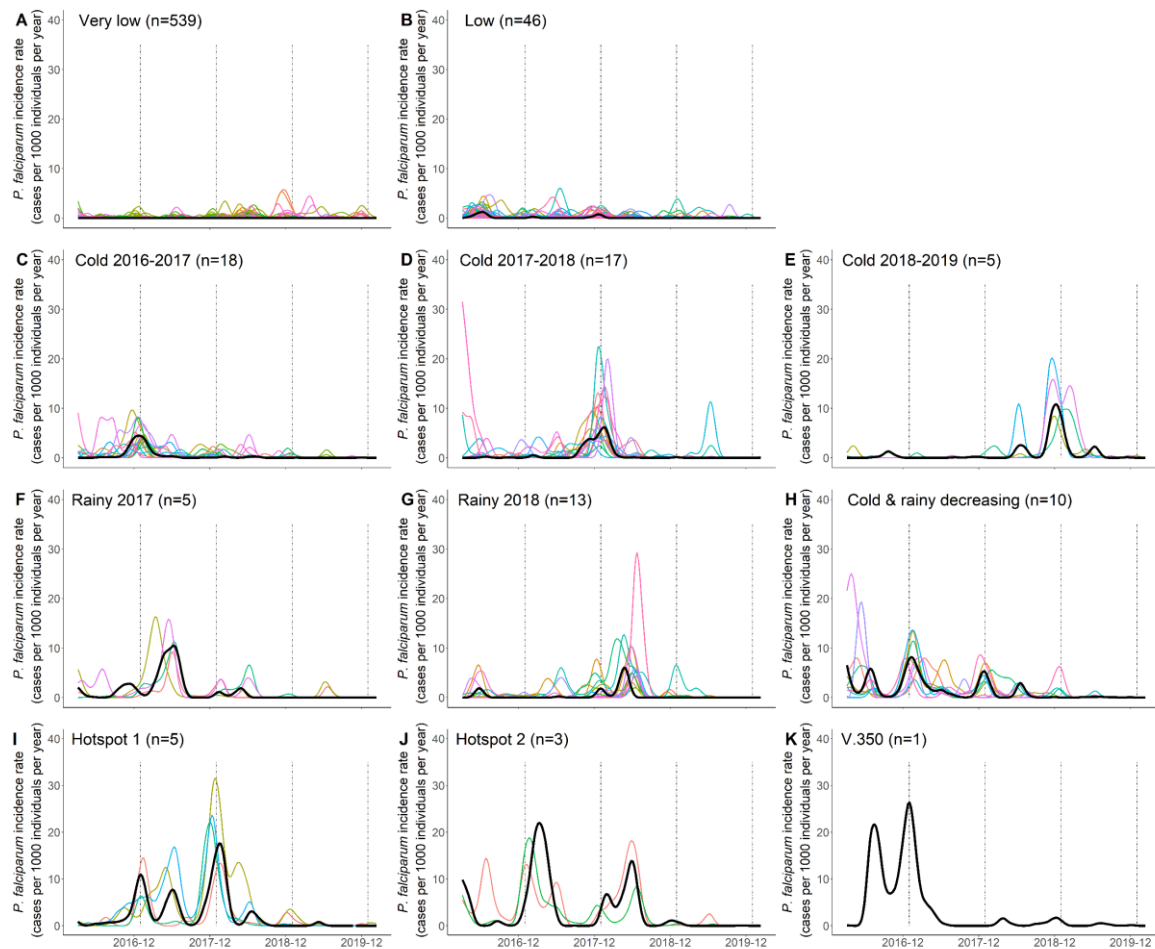


Table 2. Comparison between WHO stratification and temporal dynamic clustering for *P. falciparum*. The number of villages for each cluster/stratum is presented (TA: transmission area).

	API stratification					TOTAL
	Free TA	Potential TA	Low TA	Moderate TA	High TA	
Very low	317	145	1	22	54	539
Low	0	22	0	3	21	46
Cold 2016-2017	0	6	0	0	12	18
Cold 2017-2018	0	6	0	2	9	17
Cold 2018-2019	0	0	0	0	5	5
Rainy 2017	0	1	0	0	4	5
Rainy 2018	0	5	0	2	6	13
Cold & rainy decreasing	0	4	0	0	6	10
Hotspot 1	0	2	0	0	3	5
Hotspot 2	0	0	0	0	3	3
V. 350	0	0	0	0	1	1
<b>TOTAL</b>	<b>317</b>	<b>191</b>	<b>1</b>	<b>29</b>	<b>124</b>	<b>662</b>



366  
367  
368  
369  
370  
371  
372  
373  
374  
375  
376  
377  
378  
379  
380  
381  
382  
383  
384  
385  
386  
387  
388  
389  
390  
391  
392  
393  
394  
395  
396  
397  
398  
399  
400  
401  
402  
403  
404  
405  
406  
407  
408  
409  
410  
411

Figure 3. *P. vivax* clustering. Temporal dynamic clustering identified eleven clusters. Black line corresponds to the central village (medoid) of each cluster. Coloured lines represent functional incidence rate of all villages included in the cluster across study period. When clusters contained only one village, only the medoid (black line) is presented corresponding to the time series of the village.

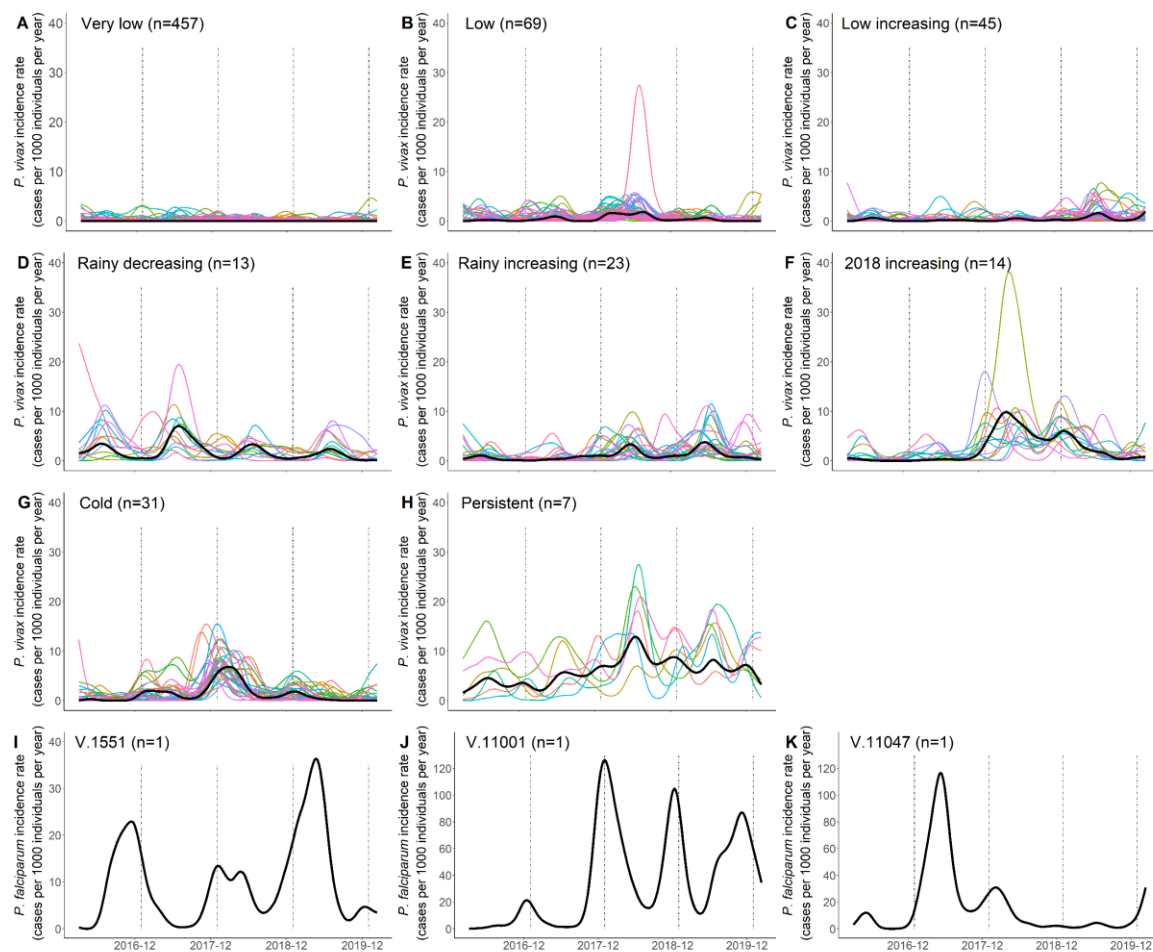
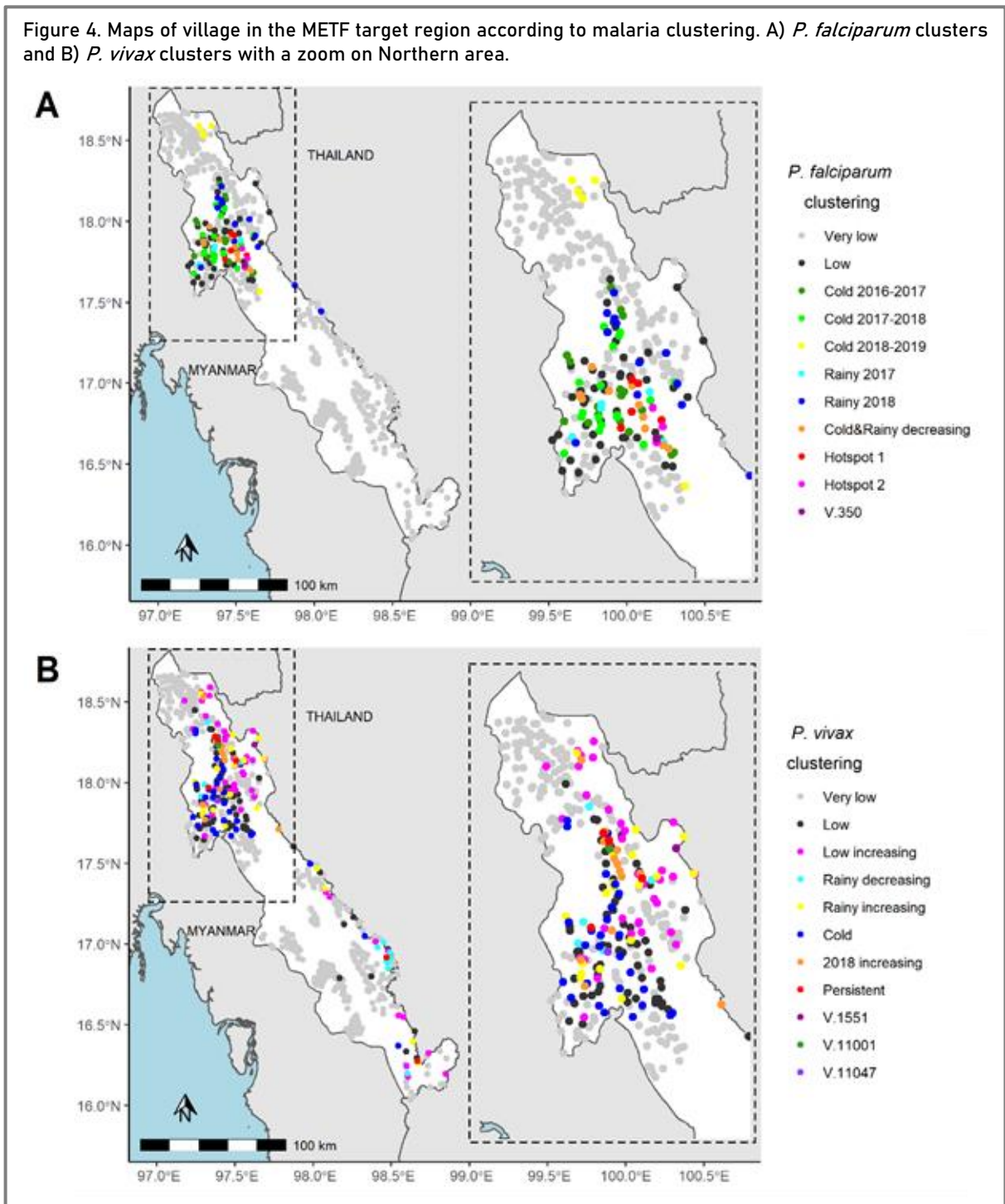


Table 3. Comparison between API stratification and temporal dynamic clustering for *P. vivax*. The number of villages for each cluster/stratum is presented (TA: transmission area).

		API stratification					TOTAL
		Free TA	Potential TA	Low TA	Moderate TA	High TA	
Temporal dynamic clustering	Very low	120	103	1	38	195	457
	Low	0	1	0	0	68	69
	Low increasing	0	0	0	0	45	45
	Rainy decreasing	0	0	0	0	13	13
	Rainy increasing	0	0	0	0	23	23
	Cold	0	0	0	0	31	31
	2018 increasing	0	0	0	0	14	14
	Persistent	0	0	0	0	7	7
	V. 1551	0	0	0	0	1	1
	V. 11001	0	0	0	0	1	1
	V. 11047	0	0	0	0	1	1
TOTAL		120	104	1	38	399	662

412  
413  
414  
415  
416  
417  
418  
419  
420  
421  
422  
423  
424  
425  
426  
427  
428  
429  
430  
431  
432  
433  
434  
435  
436  
437  
438  
439  
440  
441  
442  
443  
444  
445  
446  
447  
448



### 449 *Sensitivity analysis*

450 In order to address the wide range of incidence in the high transmission category of the API  
451 stratification, we split this category by quartiles: 5-10, 10-30, 30-100,  $\geq 100$ . We compared this 6-  
452 category API stratification to the temporal dynamic clustering from 2016 to 2019 (Sup. Fig. 4-5). 6-  
453 category stratification distinguished villages according to amplitude, some annual trends and no  
454 seasonality. The “Very low” clusters stood out from the others considering API categories (i.e. incidence  
455 amplitude). For *P. vivax*, the “2018 increasing” and “Rainy decreasing” clusters were identical

456 considering API categories. For *P. falciparum*, “Cold 2017–2018” and “Rainy 2017” clusters or “Cold 2018–  
457 2019” and “Rainy 2018” were also similar.  
458  
459

## 460 Discussion

461 Based on WHO recommendations, stratification on API (combining *P. falciparum* and *P. vivax*)  
462 incidence at village level in 2019 identified 54.7% of the villages in a moderate or high transmission  
463 area. According to national guidelines, early diagnostic and treatment should be reinforced with  
464 preventive measures in those stratum representing 564 villages.<sup>7</sup> Analyses distinguishing *Plasmodium*  
465 species showed that only 18.4% of the villages still had moderate or high *P. falciparum* transmission.  
466 It is consistent with global analysis showing that the proportion of cases attributable to *P. vivax*  
467 increased as *P. falciparum* incidence declined.<sup>22</sup> In co-endemic countries, distinct analysis according  
468 to parasite species is necessary to adapt species-specific interventions. Moreover, in a *P. falciparum*  
469 pre-elimination setting, combined *P. vivax* survey could inform about *P. falciparum* receptivity (i.e. due  
470 to longer persistence) useful to target surveillance and prevent resurgence.  
471

472 Even by considering *Plasmodium* species, API-based stratification pooled villages belonging to the  
473 *P. falciparum* hotspot cluster and low incidence patterns together, and all *P. vivax* dynamic patterns  
474 identified in the high transmission area stratum. API-based stratification could lead to coarse targeting  
475 interventions because of an insufficient discriminating stratification. By considering incidence past-  
476 years evolutions (amplitude level, tendency) and seasonality variations (i.e. intra-annual variability),  
477 the temporal dynamic clustering was more discriminant and proved to be more adapted to allocate  
478 surveillance and intervention. The clustering allowed to identify villages where additional measures  
479 are necessary (e.g. increasing tendency, persisting high incidence, recently reach zero cases), or on  
480 the contrary the one where existing interventions appear sufficient (e.g. low incidence decreasing)  
481 (Details in table 4).<sup>7</sup> It also identified intra-annual patterns and distinguished villages with one or two  
482 annual peaks, and their seasonality. This could be exploited to adapt supplies and community  
483 engagement towards preventive behaviours. It is also of interest to identify transmission bottlenecks  
484 and deployed sustainable elimination strategies by highlighting low transmission period.<sup>23</sup> The  
485 temporal dynamic clustering provided rich information about malaria dynamics, which could not be  
486 obtained through a simple, or a more complex stratification on API. Sensitivity analyses were  
487 conducted by dividing the high transmission stratum in subcategories and considering all API values  
488 over the 2016–2020 periods, without equalling the precision of the DTW metric (i.e. seasonality with  
489 time lag) (Sup. Fig. 4, 5)  
490

491 This study presented several strengths. First, the unique dataset collected by the METF community-  
492 based MP network allowed studying malaria incidence at an unprecedented granularity (village-scale)  
493 in the GMS. Beyond identifying the northern area of the region with the highest malaria burden (already  
494 shown elsewhere<sup>8,10</sup>), clustering highlighted localized groups of few villages relevant for operation  
495 planning. *P. falciparum* and *P. vivax* dynamics also could be studied separately thanks to data richness.  
496 Second, we adapted existing methods into a straightforward, step-by-step analysis workflow allowing  
497 the exploration of the temporal dynamics of a large number of time series simultaneously without  
498 assuming stationarity. An open-access script makes methodology implementation simple and  
499 repeatable in other contexts (Sup. Met. 1).  
500

501  
502  
503  
504  
505  
506  
507  
508  
509  
510  
511  
512  
513  
514  
515  
516  
517  
518  
519  
520  
521  
522  
523  
524  
525  
526  
527  
528  
529  
530  
531  
532  
533  
534  
535  
536  
537  
538  
539  
540  
541  
542  
543  
544  
545  
546

Table 4. Surveillance and intervention recommendations according to API-based stratification (AS) and temporal dynamic clustering (TDC).

Stratification	Malaria epidemiology	Surveillance and intervention recommendations
AS & TDC	Zero cases for few years	Passive surveillance
AS & TDC	Recently reach zero cases	Active surveillance (e.g. mobile team)
TDC	Low incidence with a decreasing tendency	No additional measures than existing ones
TDC	Low incidence with an increasing tendency	Additional interventions (e.g. reinforce preventive measure, early diagnostic & treatment)
TDC	Persisting high incidence	Additional interventions (e.g. reinforce preventive measure, early diagnostic & treatment, mass intervention)
TDC	Single village with specific dynamics & high incidence	Investigation

This study presented several limits. Functional transformation smoothing was necessary to transform series into continuous function and to optimize DTW algorithm.<sup>15</sup> Because MP opened gradually, data was excluded to obtain a set of observations over the same calendar period. In total 395 villages with late MP opening were excluded. However, these villages had in majority extremely low malaria incidence (4.3% villages with >5 *P. falciparum* case/year and 12.7% with >5 *P. vivax* case/year). Likewise, the first months of MP activity were excluded for MP opening earlier than the date chosen to initiate the study. This represented 12 months in average and may have prevented from identifying *P. falciparum* incidence patterns where it decreased quickly after providing access to diagnosis and treatment.

Second, clustering analysed only clinical malaria incidence and thus transmission characteristics. According to WHO guidelines, taking into account malaria receptivity will improve this clustering. Combining *P. falciparum* and *P. vivax* analysis brings some information about receptivity, but this should to be completed with more detailed data including environmental characteristics.

Finally, smaller towns could increase the variance of the incidence. It is a general concern with incidence estimation. Nevertheless, PAM clustering discriminated single outliers with a unique dynamic (e.g. Fig 3. I-K). It highlights villages where specific investigation is necessary (to understand if the unique profile identified corresponds to a truly specific situation or to correct potential data errors)."

The method proposed here provides a thorough tool to exploit longitudinal routine case data and extract an untapped wealth of information for operational planning, allowing to gauge trends, seasonality shifts or periodic outbreaks. We applied it to a fine-grained village-level malaria incidence dataset. This approach relies on village-level data yet unavailable in many settings. Our method could be used to identify longitudinal incidence patterns at coarser scale in a country-wide approach (e.g. village tract or health area). WHO "high burden to high impact" approach promotes targeting areas where malaria burden is highest, leading to stratification beyond district level, e.g. health areas or health facility catchment areas.<sup>24,25</sup> Other infectious diseases with highly heterogeneous dynamics driven by multiple factors could also be analysed in this workflow.

In conclusion, to be efficient, control and intervention planning need to take into account fine description of malaria dynamics. More sophisticated stratification than API over one year is needed to characterize it. The temporal dynamic clustering is an adapted methodology to support malaria surveillance and intervention planning which could be applied to a large number of spatial units at

547 different scales (health area, health district or region levels) in countries of the GMS, and in other  
548 regions of the world, particularly where malaria transmission is highly seasonal (Sahel, Southern  
549 Africa...).

## 551 Acknowledgments

552 The authors thank the people of Karen/Kayin State whose engagement and participation to the  
553 programme was a key element of success. We acknowledge the hard work, dedication and continuous  
554 support of all staff, collaborators and colleagues who made this project possible and contributed to  
555 implementing it up to the most remote communities. SMRU is part of the Mahidol Oxford University  
556 Research Unit, supported by the Wellcome Trust of Great Britain.

## 558 References

- 559 1. World Health Organization. Global Malaria Programme. A framework for malaria elimination.  
560 108 <https://www.who.int/publications/i/item/9789241511988> (2017).
- 561 2. Das, S., Muleba, M., Stevenson, J. C., Pringle, J. C. & Norris, D. E. Beyond the entomological  
562 inoculation rate: Characterizing multiple blood feeding behavior and *Plasmodium falciparum*  
563 multiplicity of infection in *Anopheles* mosquitoes in northern Zambia. *Parasites and Vectors*  
564 10, 1–13 (2017).
- 565 3. Yukich, J. O., Lindblade, K. & Kolaczinski, J. Receptivity to malaria: meaning and measurement.  
566 *Malar. J.* 21, 1–13 (2022).
- 567 4. Cui, L. *et al.* Malaria in the Greater Mekong Subregion: Heterogeneity and complexity. *Acta*  
568 *Trop.* 121, 227–239 (2012).
- 569 5. Imwong, M. *et al.* The spread of artemisinin-resistant *Plasmodium falciparum* in the Greater  
570 Mekong subregion: a molecular epidemiology observational study. *Lancet Infect. Dis.* 17, 491–  
571 497 (2017).
- 572 6. Imwong, M. *et al.* Molecular epidemiology of resistance to antimalarial drugs in the Greater  
573 Mekong subregion: an observational study. *Lancet Infect. Dis.* 20, 1470–1480 (2020).
- 574 7. National Malaria Control Programme. National Plan For Malaria Elimination In Myanmar 2016  
575 - 2030. 28, 3 (2016).
- 576 8. World Health Organization. External evaluation of the National Malaria Control Programme  
577 Myanmar: 6–19 March 2016. (2017).
- 578 9. Parker, D. M. *et al.* Scale up of a *Plasmodium falciparum* elimination program and surveillance  
579 system in Kayin State, Myanmar. *Wellcome Open Res.* 2, 1–20 (2017).
- 580 10. Landier, J. *et al.* Effect of generalised access to early diagnosis and treatment and targeted  
581 mass drug administration on *Plasmodium falciparum* malaria in Eastern Myanmar: an  
582 observational study of a regional elimination programme. *Lancet* 391, 1916–1926 (2018).
- 583 11. Shoklo Malaria Research Unit. Malaria Elimination Task Force, Activity Report Update May  
584 2014–December 2019. 41 (2020).
- 585 12. The Republic of the Union of Myanmar. *Census Atlas Myanmar - The 2014 Myanmar Population*  
586 *and Housing census.* (2017).
- 587 13. World Health Organization. Malaria surveillance, monitoring & evaluation: a reference manual.  
588 (2018).
- 589 14. Dieng, S. *et al.* Application of Functional Data Analysis to Identify Patterns of Malaria Incidence  
590 , to Guide Targeted Control Strategies. *Int. J. Environ. Res. Public Heal.* 17, 4168 (2020).
- 591 15. Deriso, D. & Boyd, S. A general optimization framework for dynamic time warping. *arXiv* 1–23  
592 (2019).
- 593 16. Ramsay, J., Hooker, G. & Graves, S. *Functional Data Analysis with R and MATLAB.* (Springer  
594 New York, 2009). doi:10.1007/978-0-387-98185-7.
- 595 17. Giorgino, T. Computing and visualizing dynamic time warping alignments in R: The dtw  
596 package. *J. Stat. Softw.* 31, 1–24 (2009).

- 597 18. Sakoe, H. & Chiba, S. Dynamic Programming Algorithm Optimization for Spoken Word  
598 Recognition. *IEEE Trans. Acoust. 26*, 43–49 (1978).  
599 19. Christian Hennig, Marina Meila, Fionn Murtagh, R. R. *Handbook of cluster analysis*. (2016).  
600 20. Leonard Kaufman, P. J. R. *Finding Groups in Data: An Introduction to Cluster Analysis* | Wiley.  
601 (2005).  
602 21. Montero, P. & Vilar, J. A. TSclust: An R package for time series clustering. *J. Stat. Softw.* 62, 1–  
603 43 (2014).  
604 22. Battle, K. E. *et al.* Mapping the global endemicity and clinical burden of Plasmodium vivax,  
605 2000–17: a spatial and temporal modelling study. *Lancet* 394, 332–343 (2019).  
606 23. Landier, J., Rebaudet, S., Piarroux, R. & Gaudart, J. Spatiotemporal analysis of malaria for new  
607 sustainable control strategies. *BMC Med.* 16, 2–5 (2018).  
608 24. Health Organization, W. High burden to high impact: A targeted malaria response. (2018).  
609 25. Ferrari, G. *et al.* A malaria risk map of Kinshasa, Democratic Republic of Congo. *Malar. J.* 15,  
610 27 (2016).  
611

## 612 Contributors

613 JL and JG designed the study. EL, JL and JG designed the analysis plan. EL developed the statistical  
614 analysis framework and conducted the analysis, under the supervision of JG, and with methodological  
615 contributions of SD and LL concerning functional transformation. AT, JR, JL, FN, GD supervised METF  
616 program. AT, JR, JL collected data. FN, VH, FG, GD, JR, AT, JG, SR and JL helped to the interpretation  
617 of the findings. EL wrote the first draft of the manuscript with contributions of JL, JG and SR. All authors  
618 contributed to review the analysis, wrote the manuscript and approved the final manuscript.

## 619 Funding

620 The METF program was supported by the Bill & Melinda Gates Foundation (OPP1117507), the Regional  
621 Artemisinin Initiative (Global Fund against AIDS, Tuberculosis and Malaria), and the Wellcome Trust.  
622 This study were part of the EASIMES program funded by the Regional Artemisinin Initiative 2  
623 Elimination project (RAI2E operational research QSE-M-UNOPS-SMRU-20864-007-56). This research  
624 was funded in whole, or in part, by the Wellcome Trust Thailand/Laos Major Overseas Program  
625 Renewal [grant number 106698]. For the purpose of open access, the author has applied a CC BY public  
626 copyright license to any Author Accepted Manuscript version arising from this submission. The funding  
627 body had no role in the design of the study and collection, analysis, and interpretation of data and in  
628 writing the manuscript.

## 629 Availability of data and materials

630 The data analysed for this study are available upon request to the Mahidol Oxford Tropical Medicine  
631 Research Unit data access committee: [https://www.tropmedres.ac/units/moru-bangkok/bioethics-  
632 engagement/data-sharing](https://www.tropmedres.ac/units/moru-bangkok/bioethics-engagement/data-sharing).

633 An open-accessed R script is available to facilitate methodological implementation of the temporal  
634 dynamic clustering (Sup. Met. 1).

## 635 Abbreviation

636 CI: conditional intra-class inertia; DTW: dynamic time warping; GMS: Greater Mekong Subregion; I:  
637 intra-class inertia; MDA: mass drug administration; METF: Malaria Elimination Task Force; MP: malaria

638 post; NMCP: National Malaria Control Program; PAM: Partitioning around medoids; TA: Transmission  
639 area; WHO: World Health Organization.

640

## 641 **Declarations of interest**

642 All authors declare no competing interests.

643